RESEARCH PAPER

Evaluating Corrosion and Wear Resistance of Ni-Fe(Si-Ti)C Nanocomposite Coating

Mohadeseh Karimi[1], Mohammad Hossein Enayati[1], Fatemehsadat Sayyedan[2,*]

* *sayyedan@um.ac.ir*

[1] Department of Materials Engineering, Isfahan University of Technology, Isfahan 8415683111, Iran
[2] Department of Materials Science and Engineering, Faculty of Engineering, Ferdowsi University of Mashhad, Mashhad 917751111, Iran

Received: February 2025 **Revised: December 2025** **Accepted: December 2025**
DOI: 10.22068/ijmse.3922

Abstract: *This study aimed to optimise the current density and carbide concentration during the electrodeposition of a Ni-Fe(Si-Ti)C nanocomposite coating on AISI 304 stainless steel. The optimal current density in each electrolyte was determined using scanning electron microscope (SEM) images and energy-dispersive spectroscopy (EDS) analysis. Corrosion behavior and wear resistance of the optimized coatings were examined using a TOEFL polarization test in 3.5 wt.% NaCl solution and ball-on-disk apparatus, respectively. The values of 30 mA/cm^2 and 10 mA/cm^2 were obtained to be the optimal current densities for electrolytes containing 6 g/L and 12-18 g/L double carbide, respectively. Electrochemical measurements declared that the corrosion rate decreased from 0.0829×10^{-5} mA/cm^2 to 0.0208×10^{-5} mA/cm^2 with increasing the concentration of carbide in the electrolyte from 6 g/L to 18 g/L. Moreover, the substrate's friction coefficient was found to be significantly higher than that of the coated samples.*

Keywords: *Electrodeposition, SiC, TiC, Corrosion resistance, Wear resistance.*

1. INTRODUCTION

Appropriate surface modification can either prevent or delay damage to engineering parts. The process of choosing the best way to create distinctive surface features is complicated, as it requires adjusting a range of characteristics and qualities. Furthermore, selecting an appropriate procedure generally requires consideration of economic and environmental factors [1].

Many surface coating techniques have been introduced to improve surface quality, and electro-deposition is considered a simple, cost-effective process that produces a homogeneous, dense coating with good adhesion to the substrate material, generally metals/alloys. Several benefits, including homogeneous particle dispersion, low cost, faster deposition rates, applicability to variously shaped substrates, process continuity, and flexibility in deposition conditions, have made electrodeposition a major approach for producing composite coatings [1-5].

Nickel (Ni) and related alloys have attracted significant attention as coating materials due to their superior corrosion and wear resistance. The electrodeposition of Ni-based coatings accounts for around 12% of global Ni usage [6]. In addition to pure Ni coatings, the electrodeposition process can produce Ni-based composite coatings. Carbides (SiC, TiC, and B_4C), nitrides (AlN, TiN, Si_3N_4, and BN), oxides (Al_2O_3 and GO), Borides (ZrB_2, TiB_2, and CrB_2), solid lubricants (graphite, BaF_2, and MoS_2), nanorods, nanotubes, and nanowires are some particles that can be employed as the secondary phase in composite coatings [7]. Ni-based coatings can be used in various applications such as aerospace, automotive, marine, medical, electronics, instrumentation, machine tool, and lock industries [3, 8].

The Ni-Fe coating is designed to reduce manufacturing costs while providing soft magnetic properties, high electrical conductivity, adequate corrosion resistance, and unique optical properties [9]. Lee et al. [10] created a nanocrystalline Ni-Fe coating and found that the electrolyte temperature had a significant impact on the phase structure. To enhance the magnetic and electrochemical properties of Ni-Fe coatings, Pavithra et al [11] created nanocrystalline Ni-Fe alloys. However, according to earlier literature [12], Ni-Fe alloys were not recommended for the manufacturing of MEMS (microelectromechanical systems) due to their poor mechanical properties. The inclusion of a second reinforcing phase in a composite coating affects the coating's corrosion behaviour and mechanical properties. Co-deposition of ceramic particles into the Ni-Fe matrix, such as SiC [13], TiC [14], TiO_2 [15], and Al_2O_3 [16], has been reported in many attempts.

[DOI: 10.22068/ijmse.3922]

TiC is one of the hardest carbides and could be a suitable candidate as a composite reinforcement because of its pronounced properties, namely high melting temperature (3420 K), high hardness (3200 kg/mm^2), high bending strength, low density (4.95 g/cm^2), high mechanical stiffness, high modulus, high electrical conductivity, thermal stability, and superior corrosion and erosion resistance [17]. TiC-reinforced Ni-matrix composites have been continuously improving since the 1960s due to their remarkable mechanical and physical performance, even at high temperatures, for refractory, abrasive, and structural applications [18]. Further, researchers have explored Ni–SiC composite coatings extensively, owing to their high hardness and Young's modulus, superior wear resistance, high-temperature oxidation resistance, and low cost of SiC particles [19-22]. The co-deposition mechanism of micro- and nano-SiC particles incorporated into a nickel matrix has been described by Gyftou et al. [23]. The mechanical properties of Ni–SiC nano-composites have been studied by Zimmerman et al [19]. They have been used to protect the interiors of cylinders, combustion engines, and casting moulds from friction [20].
Simultaneous application of TiC and SiC as reinforcement materials in Ni-Fe composite coatings can improve the mechanical properties of the coatings. While the effects of SiC and TiC reinforcements on the characteristics of Ni-matrix composites have been studied independently, there are no reports focusing on the effects of TiC and SiC reinforcements on the properties of Ni-Fe nano-composite coatings. The aim of this research was to investigate the microstructure, microhardness, wear, and corrosion resistance of Ni-Fe(Ti,Si)C nano-composite coatings prepared by co-electrodeposition.

2. EXPERIMENTAL PROCEDURES

Ni-Fe(Ti,Si)C nanocomposite was electrodeposited from Watts' nickel electrolyte containing Fe_2SO_4 (as iron source), SDS (for better dispersion), and suspended TiC and SiC nanoparticles with an average diameter of 40-60 nm. The mass ratio of TiC:SiC was adjusted to 6:4. To create a more stable suspension of TiC and SiC powders, the synthesised bath was treated with ultrasound for 30 min and mechanically stirred for 24 h before use. Mechanical stirring was also maintained throughout the electrodeposition process.
The composition of the electrodeposition bath and process parameters are summarised in Table 1. AISI 304 stainless steel was used as the cathode with a surface area of 2.5 cm^2. Table 2 presents the chemical composition of the substrate. A nickel electrode (2×1×10 cm^3) was used as the anode. The distance between electrodes was adjusted to 2 cm. The specimens were cold-mounted and mechanically polished to 1200 grit using abrasive SiC papers. To achieve surface activation, the substrates were cleaned with ethanol for 10 min and then etched in 18 vol.% HCl for 50 s. It is noteworthy that a combination of anodic and cathodic treatments may be necessary to reach a high degree of adhesion, typically in stainless steel and nickel-based alloys. Accordingly, anodic treatment in 70 vol.% H_2SO_4 at 107 mA/cm^2 for 3 min and cathodic treatment in the strike solution (240 g/L $NiCl_2$, 120 ml/L HCl) at 108 mA/cm^2 for 2 min were conducted. The specimens were rinsed in distilled water and immediately placed in the electrodeposition bath. The electrodeposition process was performed at 6, 12, and 18 g/L carbide concentration and at different current densities to investigate the effects of carbide content and current density on the microstructure, wear, and corrosion behaviour of the coatings. Samples' codes are listed in Table 3. The surface morphology of the coatings was studied by a scanning electron microscope (SEM, Philips XL30) equipped with an energy-dispersive spectroscopy (EDS) analyzer.

Table 1. Electrodeposition bath composition and process parameters

Bath composition and technology	Concentration and working condition
$NiSO_4 \cdot 6H_2O$ (nickel sulfate hexahydrate)	250 g/L
$NiCl_2 \cdot 6H_2O$ (nickel chloride hexahydrate)	45 g/L
H_3BO_3 (boric acid)	40 g/L
Fe_2SO_4 (Iron III sulfate)	10 g/L
Dodecyl sodium sulfate	1 g/L
Carbide's particle	6, 12, 18 g/L
Current density	5, 10, 20, 30, 40, 50 mA/cm^2
pH	3.5-4
Temperature	55 °C
Stirrer rate	500 rpm

[DOI: 10.22068/ijmse.3922]

Table 2. Chemical composition of AISI 304 stainless steel

Element	C	Si	S	P	Mn	Ni	Cr	Mo	Ti
Wt.%	0.401	0.292	0.030	0.007	2.27	14.7	18.6	0.0404	2.6

Table 3. Samples' codes

Samples' codes	Carbide concentration (g/L)	Current density (mA/cm^2)
6-10	6	10
6-20		20
6-30		30
6-40		40
6-50		50
12-5	12	5
12-10		10
12-20		20
12-30		30
18-5	18	5
18-10		10
18-20		20
18-30		30

To evaluate the crystallite size, an X-ray diffractometer (Philips X'PERT MPD, 40 kV) with Cu Kα radiation (λ= 1.5405 Å) was utilized. The crystallite size (d) of the coating was calculated by the Scherrer Equation (2.1):

$$d= K\lambda/\beta\cos\theta \quad (2.1)$$

Where d is the average crystallite size, K is the Scherrer constant of 0.89, λ is the wavelength of X-ray radiation used, θ is the angle of diffraction, and β is the diffraction peak semi-height width (radians). The mass fraction of carbide particles in the coatings could be calculated according to the following relationships [17]:

$$W_{nC}= (M_n/M_{nC}) \times W_n \quad (2.2)$$

Where n is Si and Ti, W_{nC} is the mass fraction (%) in the composite coatings and M is the molar mass (g/mol). Was examined by energy dispersive spectroscopy (EDS) coupled to the SEM.

The Vickers microhardness (HV in kgf mm^{-2}) of Ni-Fe(Ti,Si)C nanocomposite coatings was measured using a Reichert microhardness tester under a 50 g load for 10 s, and the final values were determined as the average of 5 measurements.

The wear resistance of Ni-Fe(Ti,Si)C nanocomposite coating was examined using a ball-on-disk friction and wear tester under dry sliding conditions at room temperature. The friction coefficient was recorded automatically during the test, and worn surface morphologies of Ni-Fe(Ti, Si)C nanocomposite coatings were studied by SEM after testing.

The electrochemical investigation of the coating was performed in 3.5 wt.% NaCl solution using Potentiostat. Potentiodynamic Polarization was used to examine the corrosion behavior. The electrochemical measurements were done using a conventional three-electrode system at room temperature. The electrodeposited coating served as the working electrode, while a saturated Ag/AgCl electrode and a Pt electrode served as the reference and counter electrodes, respectively. The anodic polarisation test was carried out by scanning the samples from the cathodic region -0.25 V to the anodic region +0.25 V at a scan rate of 100 mV/min, with respect to the OCP.

3. RESULTS AND DISCUSSION

Deposition factors, such as current density, electrolyte concentration, pH, deposition time, and bath temperature, have significant effects on the physical properties of coatings generated by electrodeposition [24,25]. To test the influence of current density, the pH, temperature, and electrolyte concentration were kept constant.

Fig. 1 represents the topographical feature of the composite coating with varying carbide particle loading in the bath. This figure obviously shows a typical nodular surface morphology. It was observed that the coating morphology became smoother and denser as the current density increased [4]. Appropriate current density can substantially increase the electric field force and greatly reduce the thickness of the hydrogen revolution layer, resulting in significant incorporation of SiC and TiC nanoparticles into the Ni-Fe(Si-Ti)C nanocomposite coating.

[DOI: 10.22068/ijmse.3922]

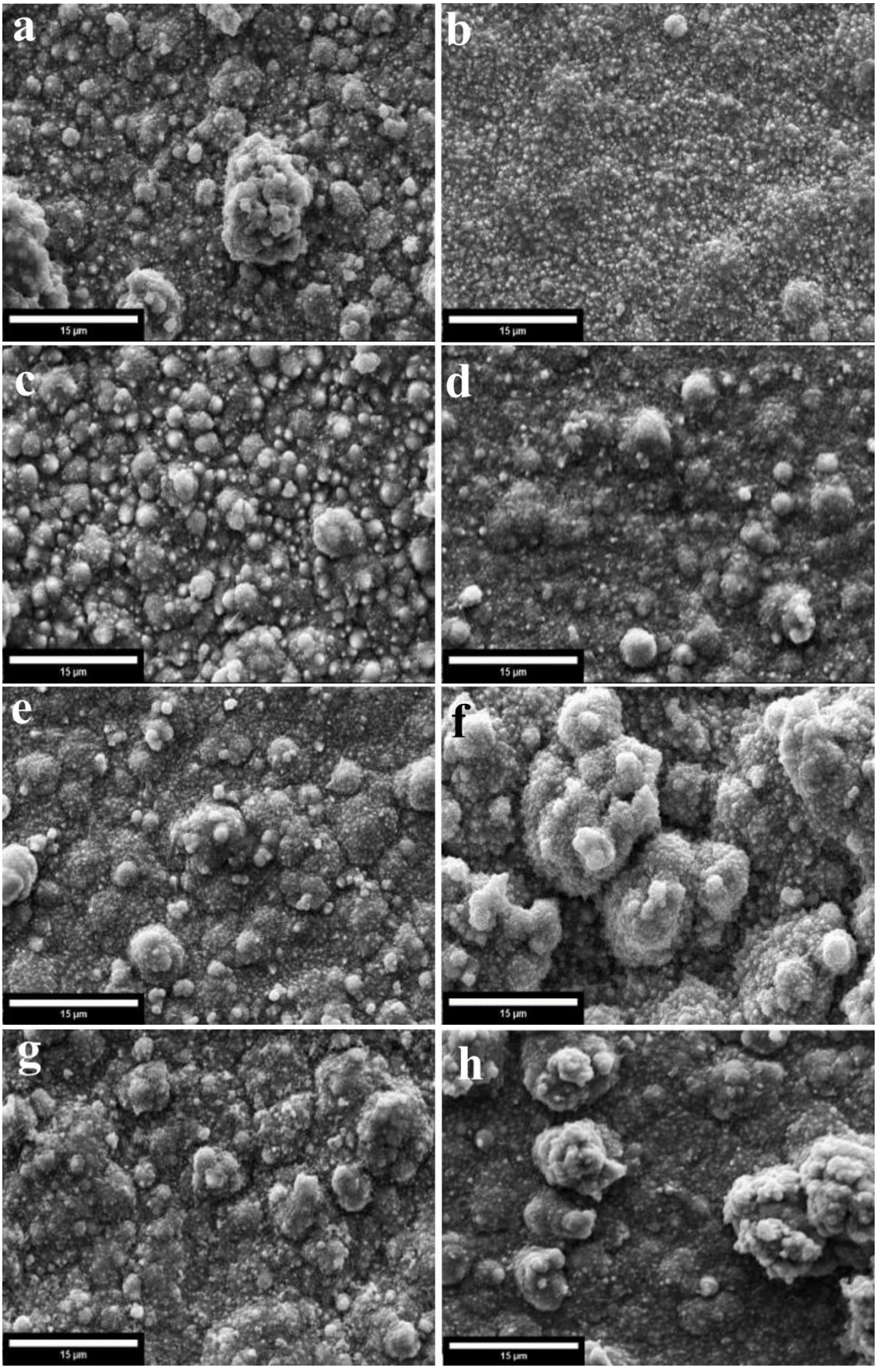

[DOI: 10.22068/ijmse.3922]

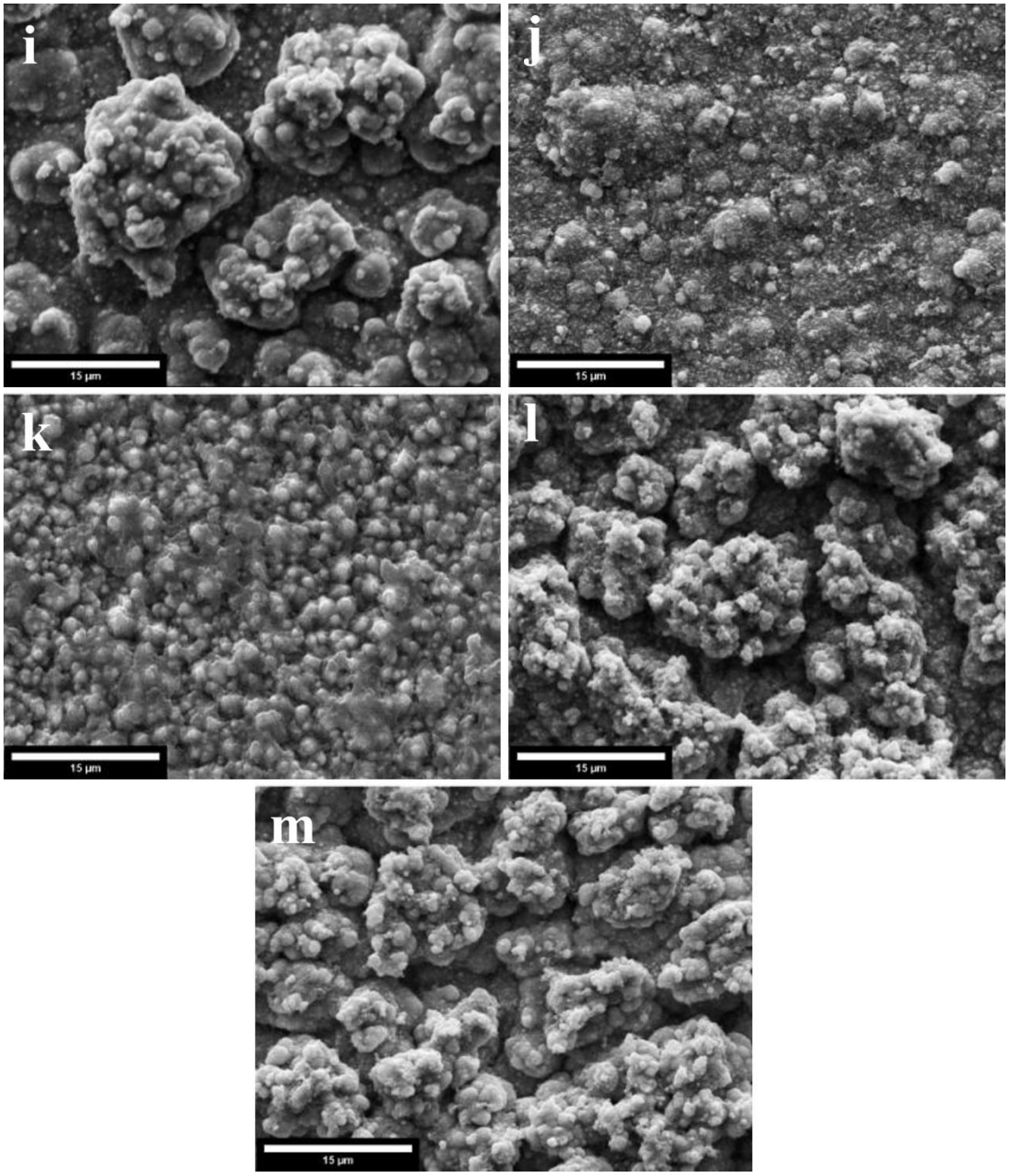

Fig. 1. SEM images of Ni-Fe(SiC-TiC) nanocomposite coating, a) 6-10, b) 6-20, C) 6-30, d) 6-40, e) 6-50, f) 12-5, g) 12-10, h) 12-20, i) 12-30, j) 18-5, k) 18-10, l) 18-20, m) 18-30

As a result, carbide nano-particles precipitated in the active nucleation sites of co-deposition and restricted nucleus development, leading to smooth, uniform, and fine morphology [15, 26]. However, by increasing the current density further, the surface morphology changed from dense and compact to rough and globular, as shown in Fig. 1. The globule size grew with further increase in current density. The distribution of Ni, Ti, Si, Fe, and C atoms was analyzed by elemental mapping attached to SEM, as shown in Fig. 2. The homogeneous dispersion of particles in the nanocomposite can be observed. Fig. 3 shows the cross-sectional SEM micrograph of samples 6-30, 12-10, and 18-10. The coating time was the same across all three samples, but the coating thickness varied. As can be seen, the interface of the Ni-Fe(Si-Ti)C coating is smooth, with no porosity and microcrack.

A typical EDS and map of the cross-section for sample 18-10 was developed in order to estimate

[DOI: 10.22068/ijmse.3922]

the chemical characterization of incorporated particles (Fig. 4). It indicated that the Ni-Fe matrix was enriched with Ti and Si elements. Also, the distribution of SiC and TiC particles was different from each other, mainly due to the different mobility of SiC and TiC particles.

The mass fraction of TiC and SiC in the composite coating with different electrolyte concentrations and a current density of 10 mA/cm^2 is presented in Fig. 5. It is obvious that increasing the particle concentration in the electrolyte has increased the incorporation of SiC and TiC particles. As the concentration of carbide particles in the coating rises in a particular range, the number of suspended particles also rises, and therefore, the number of particles transported to the cathode surface in a certain time increases. This results in a greater volume fraction of carbide particles being incorporated into the coating. This trend has been confirmed in previous literature [27-30]. The previous literature reported a descending trend for mass fraction of particles after reaching a maximum value, the trend of mass fraction of carbides maintained ascending with increasing carbide content in electrolyte, though (Fig. 5). Lee et al. [31] proposed that the maximum particles incorporated may occur at the particle concentration consistent with steady state equilibrium, where the number of incorporated particles is equal to the number of particles approaching the cathode surface.

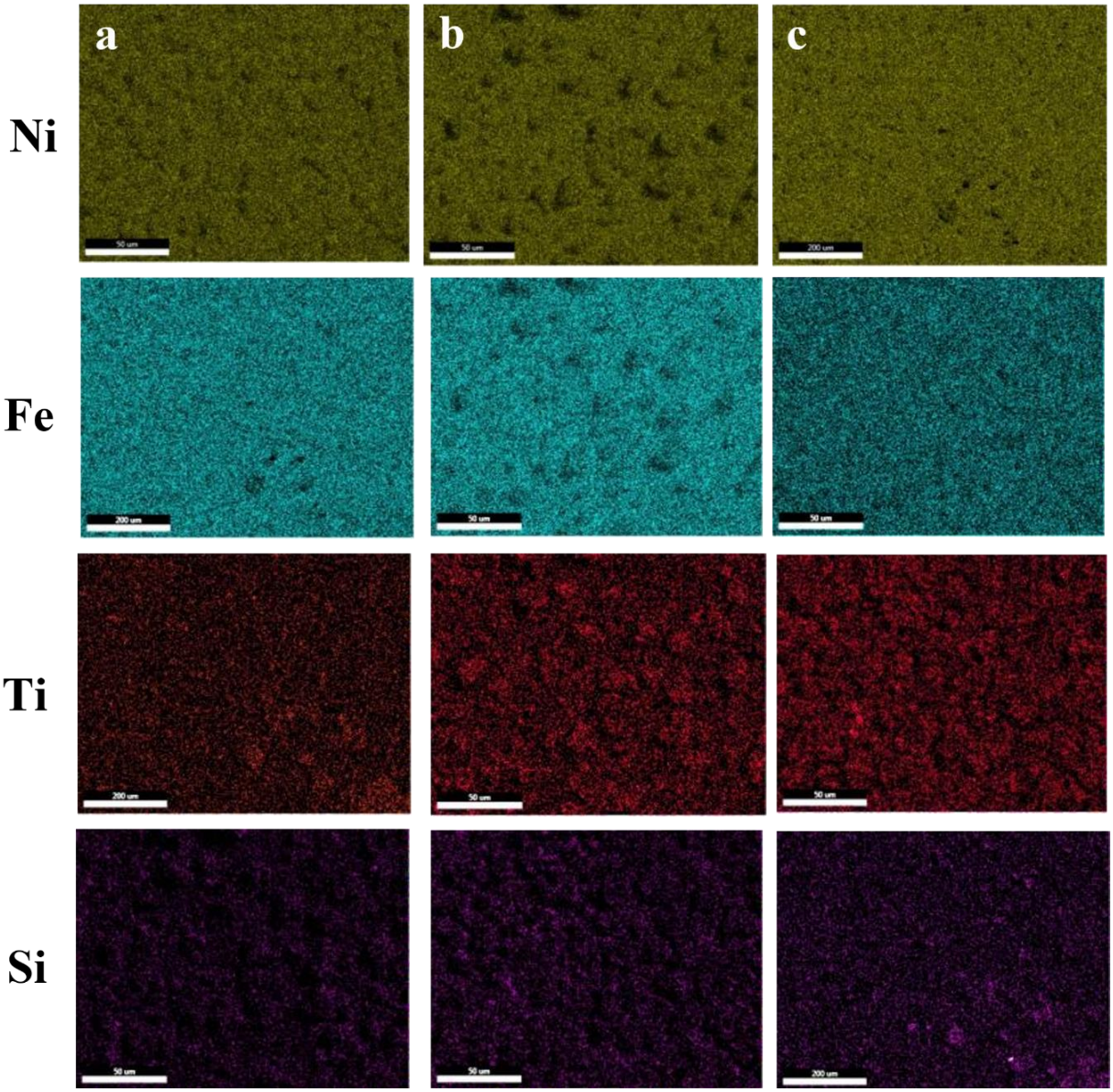

Fig. 2. Elemental mapping analysis of Ni-Fe (SiC-TiC) nanocomposite, a) 6-30, b) 12-10, c) 18-10

[DOI: 10.22068/ijmse.3922]

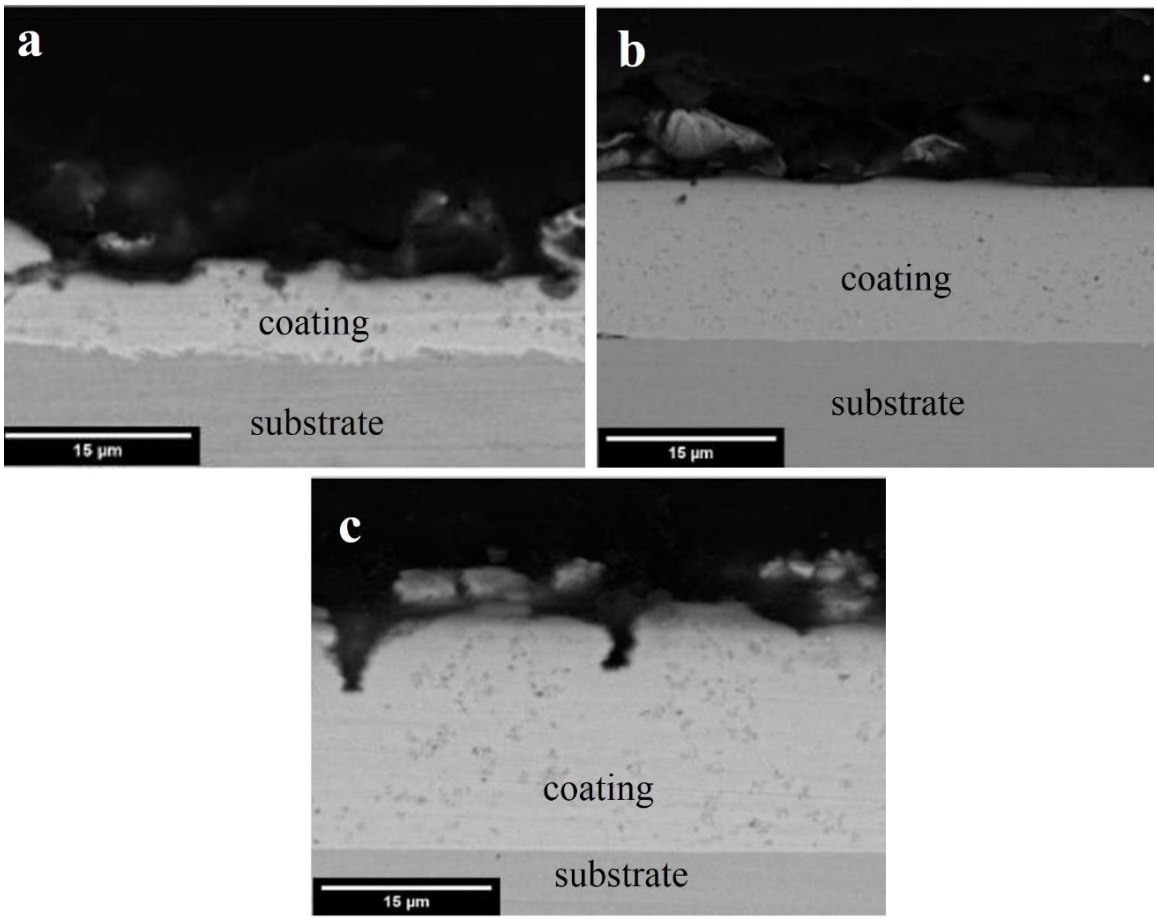

Fig. 3. Cross-sectional SEM micrographs of Ni-Fe (Si-Ti)C composite coatings: a) 6-30, b) 12-10, c) 18-10

Accordingly, in this investigation, the carbide content in the electrolyte has not yet exceeded the carbide content in the coating. As a result, with increasing carbides content in electrolyte, the mass fraction in the coating increases. The relationship between the mass fraction of TiC, SiC, and Fe in different current densities over the electrolyte concentration range from 6-18 g/L is shown in Fig. 6. As seen in Fig. 6a, the mass fraction of carbides in coating over current density increases steadily, reaching a maximum value and then decreases.

The increasing trend can be explained by the rising tendency for absorbed particles to reach the cathode surface, which is consistent with Guglielmi's model [32]. Guglielmi proposed that in the first stage, the Wonder-Waals force adsorb particles weakly at the cathode, and in the second step, the Coulomb force adsorb particles powerfully at the cathode, causing them to be immersed with the deposited metal. According to Faraday's first law, as the current density increases, the Coulomb force increases, and more SiC and TiC nanoparticles are deposited on the cathode.

As stated by Beltowska-Lehman et al. [32], the decreasing trend may be attributed to the fact that higher current density leads to faster metal matrix deposition. As a result, fewer carbide particles can be incorporated in the coating. Fig. 6b confirms this observation. It is obvious that the mass fraction of Fe increases with increasing current density.

According to the surface morphology of the coating presented in Fig. 1 and the mass fraction of carbide in Fig. 6a, 30 mA/cm^2, 10 mA/cm^2, and 10 mA/cm^2 were obtained to be the optimal current densities in 6 g/L, 12 g/L, 18 g/L carbide concentrations, respectively, which caused maximum incorporated carbide.

The Debye-Scherrer formula was used to estimate the crystallite size of the nickel film. The crystallite size, averaged across different current densities, for each electrolyte is shown in Table 4. Electrolyte composition and deposition parameters affect the grain size [33]. Increasing the carbide's concentration decreased the Ni matrix grain size. The regularly dispersed Ni embryos and SiC and TiC particles in the Ni matrix restricted the growth of the Ni

[DOI: 10.22068/ijmse.3922]

crystallite, indicating the reduction of crystallite size of the Ni matrix [17]. Carbide nanoparticles adhered to the cathode surface can also serve as nucleation sites during electrodeposition, accelerating nickel matrix nucleation. Coating growth is influenced by both nucleation and crystal growth rate [8]. Similar results were reported for Ni-SiC [34], Zn-TiO_2 [35], and Ni–ZrC [36] systems.

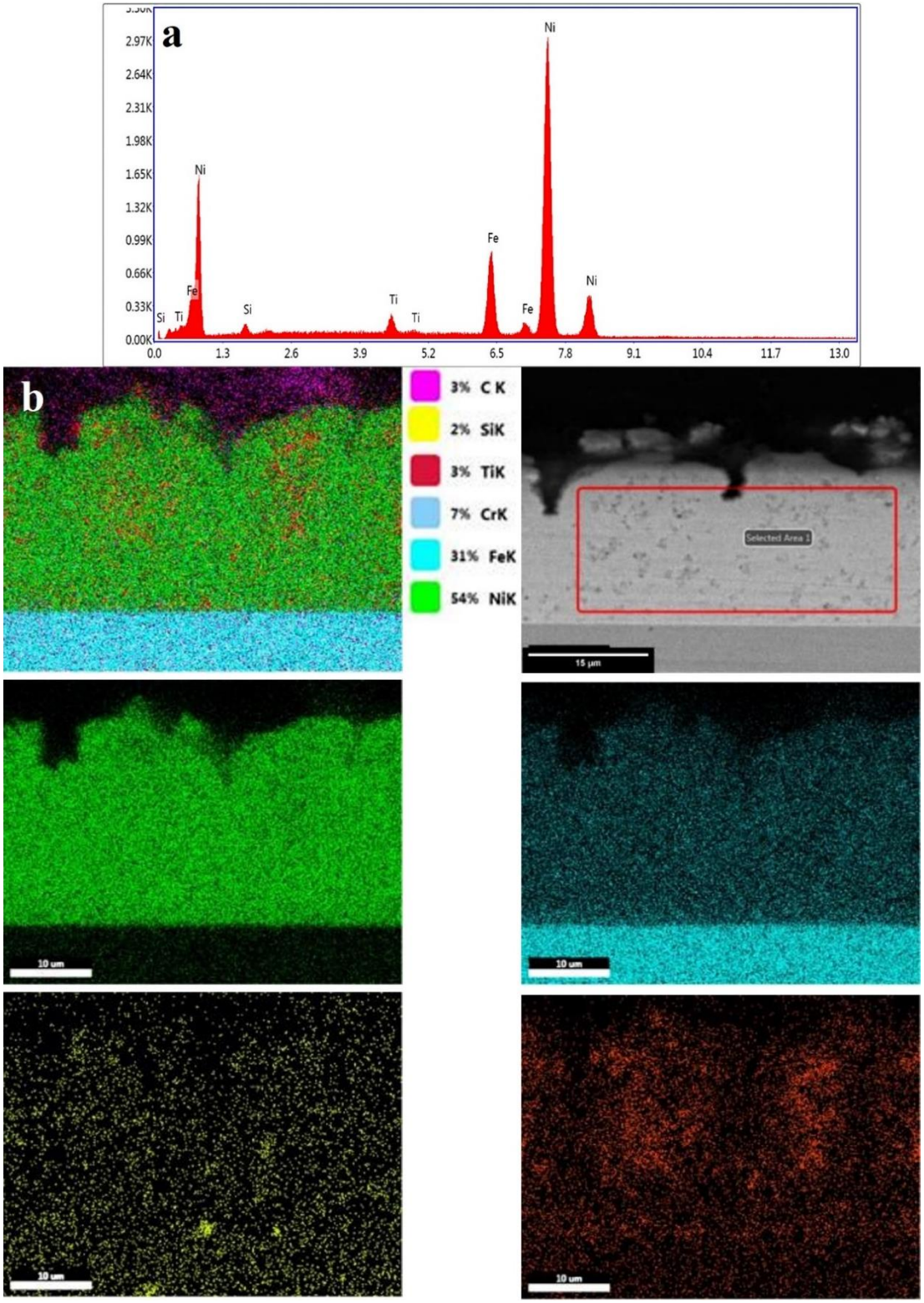

Fig. 4. a) EDS and b) elemental map analysis of Ni-Fe (Si-Ti)C composite coatings in sample 18-10

[DOI: 10.22068/ijmse.3922]

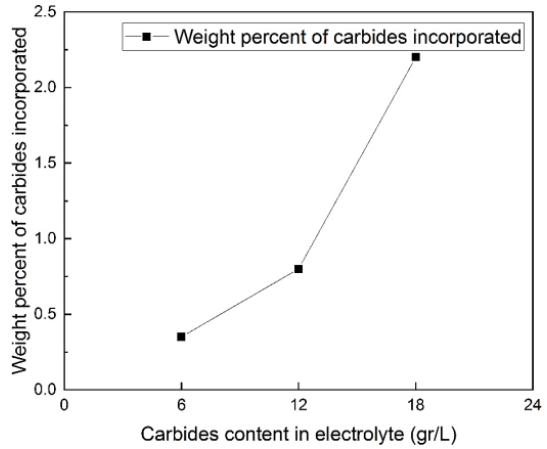

Fig. 5. The effect of carbide content in electrolyte on weight percentage of TiC and SiC carbides incorporated in the Ni-Fe (Si-Ti)C composite coating

Table 4. Crystallite size at different current densities, averaged across 6, 12, and 18 g/L carbide concentrations

Carbide concentration (g/L)	6	12	18
Crystallite size (nm)	318	250	227

Fig. 7. shows the relationship between current density and crystallite size for 18 g/L carbide concentration. A finer crystallite size was achieved by increasing the current density. This phenomenon was expected because increasing the current density increases nuclear polarisation and the production rate, ultimately leading to the development of finer crystallites [37, 38]. These results were predictable based on the general trends presented by Winand et al [13, 39]. The microhardness of the composite coating against the carbide content and crystallite size are plotted in Figs. 8 and 9, respectively. Accordingly, it is obvious that the hardness value increases with increasing carbide content in the electrolyte. Dispersion strengthening, the Orawan mechanism, and crystallite size refining are three factors that contribute to improving the coating hardness [17, 20, 21]. SiC and TiC nanoparticles placed in the nickel matrix could control the growth of nickel crystallites, followed by the plastic deformation of the matrix during loading. Higher carbide nanoparticle content leads to refinement of the crystallite size and a dispersion-strengthening effect, thereby enhancing the microhardness of the coating [20, 21]. Dislocation bowing around carbide nanoparticles, acting as dislocation pinning sites, enhances the flow stress, with the effect inversely proportional to particle dispersion, according to Orawan's hardening theory. Therefore, as the volume percentage of SiC and TiC particulates in the coating increases, particle dispersion decreases, and flow stress increases [8, 17, 19, 38].

Mo et al. [39] found that increasing the particle content refines the grain size and improves hardness and wear resistance. Nagayama et al. [13] observed that hardness increased with increasing SiC content in both heat-treated and untreated Fe-Ni/SiC composite films.

The relationship between the crystallite size and microhardness can be expressed by the Hall-Petch equation, $H = H^{\circ} + Kd^{-1/2}$, where K is a constant, d is crystallite size, H is microhardness, and H° is the intrinsic hardness of the material. This is based on the idea that crystallite boundaries act as barriers to dislocation motion, creating a dislocation pile-up and thereby increasing microhardness. Kartal et al. [18] concluded that the nickel matrix crystallite size decreased from 34.48 nm to 26.35 nm upon adding TiC reinforcement, accompanied by an increase in coating microhardness.

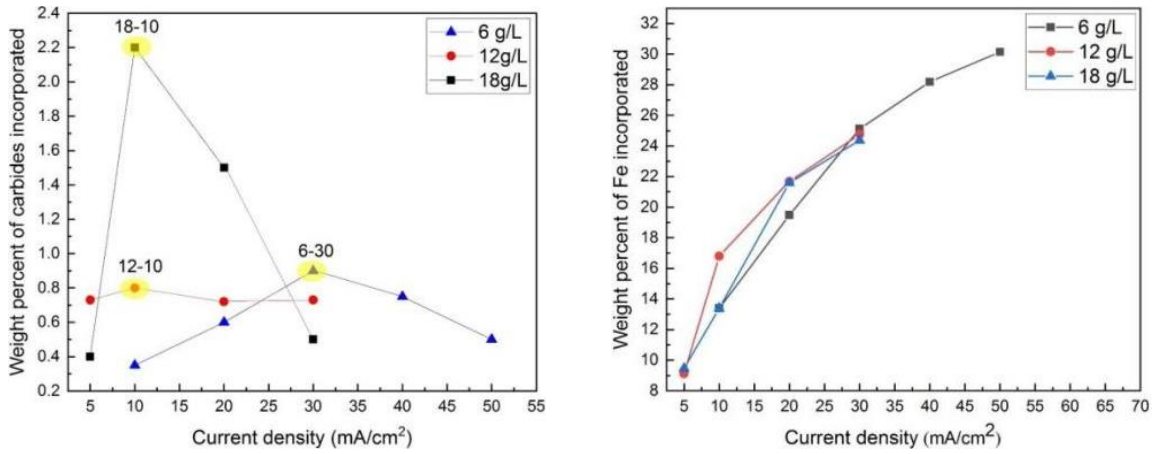

Fig. 6. The effect of current density on the weight percentage of a) TiC and SiC carbides, and b) Fe incorporated in the Ni-Fe (Si-Ti) C composite coating

[DOI: 10.22068/ijmse.3922]

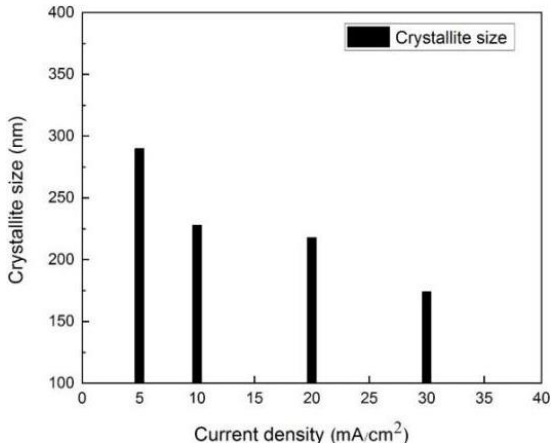

Fig. 7. The effect of current density on the Ni crystallite size of Ni-Fe (Si-Ti)C composite coatings in 18 g/L carbide concentration electrolyte

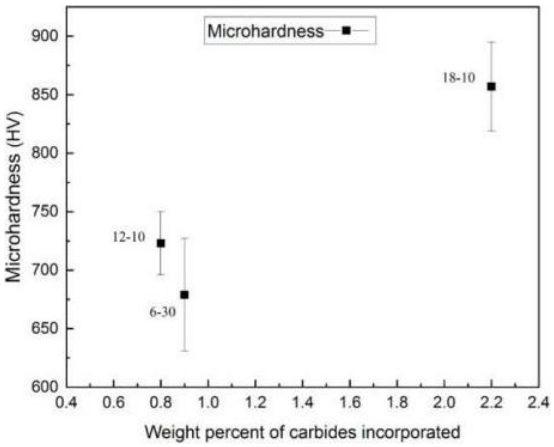

Fig. 8. The effect of the weight percentage of carbides incorporated on the microhardness of Ni-Fe (Si-Ti)C composite coatings

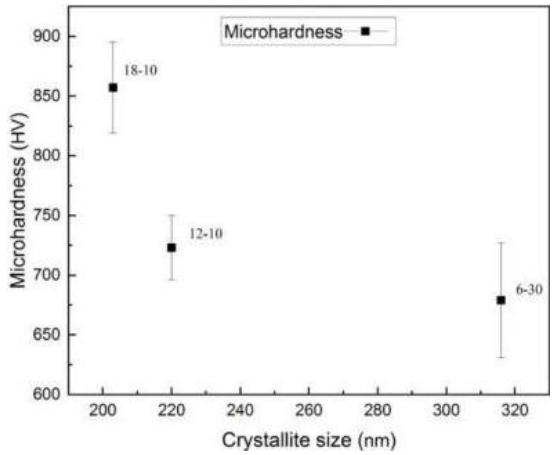

Fig. 9. The effect of crystallite size on microhardness of Ni-Fe (Si-Ti)C composite coatings

The friction coefficient of the substrate, 6-30, 12-10, and 18-10 samples versus sliding distance, obtained from pin on disc test under non-lubricated condition at room temperature is shown in Fig. 10. It was observed that in coated samples, the variations of friction coefficient decreased and became more uniform compared to the bare substrate, and sliding distance increased. TiC and SiC nanoparticle content, along with the coating's microhardness, are the major parameters that determine the friction coefficient of the Ni-Fe(Si-Ti)C nanocomposite coating [26]. The presence of a harder reinforcing phase in a ductile matrix at a specific volume fraction can reduce matrix deformation in the contact zone, thereby mitigating wear. Several studies have been conducted in this field. Gül et al. [27] used pulse electrodeposition to produce Ni-SiC composite coatings and the ball-on-disc method to assess the effect of SiC particle concentration on the coatings' wear resistance. They concluded that the wear rate was significantly reduced with increasing the SiC particle concentration in electrodeposition (from 5 g/L to 20 g/L). This was attributed to the harder coatings, grain refinement, and dispersion strengthening by adding carbide particles. Also, Jenczyk et al. [40] demonstrated that the friction coefficient increased with increasing volume fraction of coated particles in the Ni-SiC composite coatings.

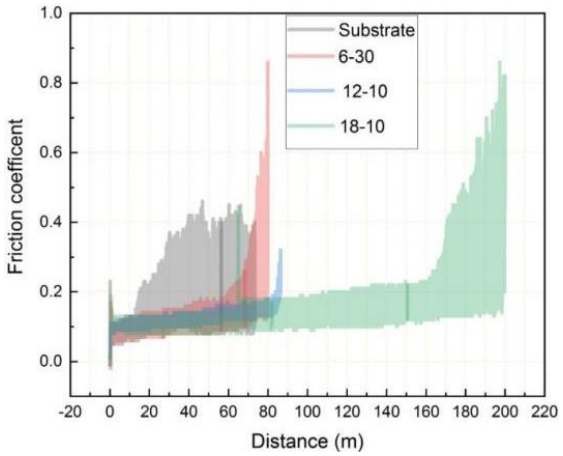

Fig. 10. Friction coefficient of the bare substrate and Ni-Fe (Si-Ti)C composite coatings in optimal samples versus distance

Figure 11 displays the surface morphologies of the bare substrate, 6-30, 12-10, and 18-10 samples under the same loading. Figure 11 (a and b) shows the substrate morphology with characteristics of adhesion wear. There are obvious plowing and delamination on the surface, along with significant wear and plastic deformation. In the Ni-Fe(Si-Ti)C surface, plastic deformation reduced gradually.

[DOI: 10.22068/ijmse.3922]

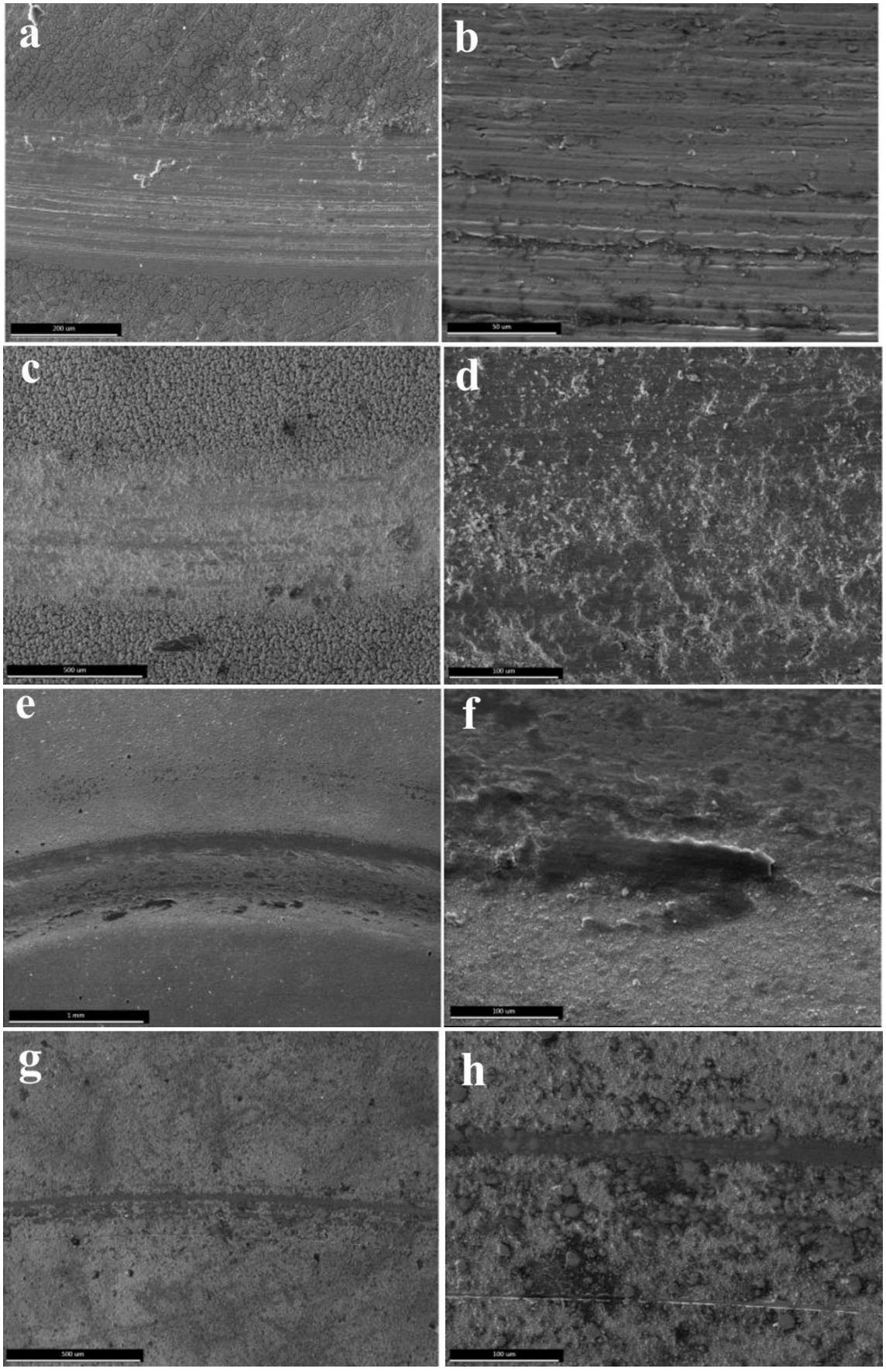

[DOI: 10.22068/ijmse.3922]

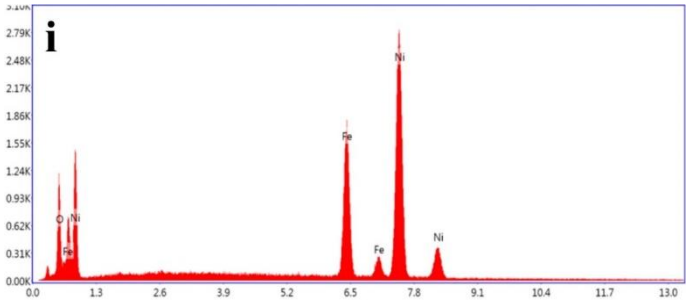

Fig. 11. Worn surface morphologies of Ni-Fe (Si-Ti)C coatings, a,b) bare substrate, c,d) 6-30, e,f) 12-10, g,h) 18-10, i) EDS of 12-10

SiC and TiC nano particles prevent plowing and the effects of wear appear as shallow grooves. Also, as SiC and TiC increase, wear scars become smoother and narrower with slight scratches. According to these observations, the dominant wear mechanism in the coated samples appears to be abrasive wear. In fact, the reinforcement particles reduce the contact area with the pin, thereby reducing the adhesion wear mechanism.

In 6-30 morphologies presented in Fig.11 (c and d), the abrasive particle is clear. The separation of materials from the coating surface in the abrasive wear mechanism is due to the presence of hard particles on the surface. The colour variation in 12-10 morphologies (Fig. 11e and 11f) demonstrated that the iron separated from the 52100 pin and adhered to the counterpart surface. The colour difference between nickel and iron has been demonstrated by Hou et al. [28]. The EDS analysis of the 12-10 specimen (Fig. 11i) confirmed the presence of iron. In addition, the presence of oxygen peaks indicated that iron was oxidising at higher temperatures in the contact zone.

Wear scar in 18-10 morphologies (Fig. 11 g and h) was smooth, and only traces of partial wear were observed. The significant amount of reinforcing phase in this coating improved the wear resistance.

Figure 12 shows the polarization curves of the bare substrate and 6-30, 12-10, 18-10 samples in 3.5 wt.% NaCl solution. The corrosion current density (i_{corr}), corrosion potential (E_{corr}), and cathodic and anodic branch slope (βc and βa) values were estimated using the Tafel extrapolation method, as shown in Table 3. Furthermore, the polarization resistance (Rp) was calculated using the Stern–Geary equation (equation 1) [42] and reported in Table 3.

Equation 1: $Rp = \frac{\beta a \times \beta c}{2.303 icorr(\beta a + \beta c)}$

As shown in Fig. 12, all graphs exhibit an active-passive transition under anodic polarisation; however, in the coated samples, the corrosion current density decreased, and the corrosion potentials shifted to more noble values, indicating improved corrosion behaviour of the bare substrate. According to Table 3, the polarization resistance of the steel substrate was 2.6 kΩ.cm^2 which increased to 180, 251 and 487 kΩ.cm^2 for 6-30, 12-10 and 18-10 coated samples, respectively.

This high corrosion resistance of the coatings could be due to several factors. The adsorption of SiC and TiC nanoparticles decreases the transport of corrosive ions to the surface. Also, uniform distribution of carbide particles in the coating can fill crevices, gaps, and micro-holes, creating a denser surface [20, 41]. Therefore, these particles act as a barrier and limit the penetration path of the corrosive media [22, 41, 44]. As shown in Table 3, the 18-10 coatings with higher wt.% carbide particles prove to be most resistant in a NaCl solution compared to other samples. As described before, the grain refinement occurred due to the incorporation of more particles, so not only the amount of carbide particles but also the change in microstructure have significantly improved the corrosion resistance of the 18-10 coated sample [45].

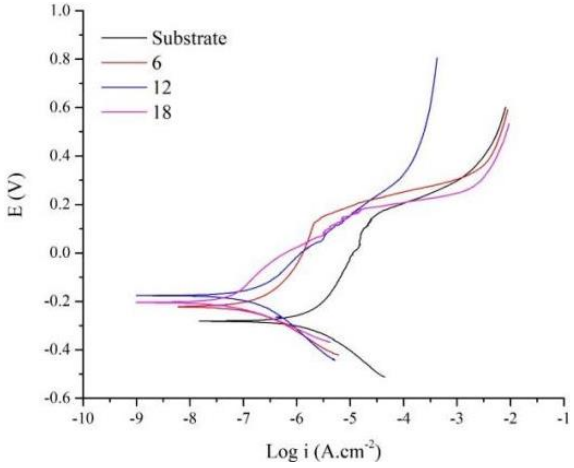

Fig. 12. Polarization curves of the bare substrate and Ni-Fe (Si-Ti)C coatings in 3.5 wt.% NaCl solution

[DOI: 10.22068/ijmse.3922]

Table 5. E_{corr}, i_{corr}, and corrosion rate for Ni-Fe (Si-Ti)C coatings in 3.5 wt.% NaCl

Code	Carbides in electrolyte (g/L)	Carbides incorporating in coating (wt.%)	E_{corr} (mV)	i_{corr} (μA/cm^2)	$^{\beta}a$ (V/dec)	$^{\beta}c$ (V/dec)	polarization resistance (kΩ.cm^2)
Substrate	-	-	-288	1.83	0.35	0.16	2.6
6-30	6	0.9	-235	0.21	0.29	0.13	180
12-10	12	0.8	-182	0.16	0.21	0.17	251
18-10	18	2.2	-208	0.05	0.20	0.07	487

4. CONCLUSIONS

In this study, a Ni-Fe(Si-Ti)C nanocomposite coating was electrodeposited on the AISI 304 stainless steel surface and optimised at different current densities and double carbide concentrations. The main results were as follows:

1. The morphology of the coating became smoother and denser with increasing the current density. However, further changes led to a shift from dense and compact to rough and globular surface morphology, with the globule size increasing.
2. The mass fraction of carbides in the coating over current density increased steadily, reaching a maximum value, and then decreased. The values of 30 mA/cm^2 for 6 g/L and 10 mA/cm^2 for 12 and 18 g/L electrolytes were chosen as the optimal current densities, resulting in the maximum incorporation of carbides.
3. Increasing the current density caused an increase in nuclear polarization and production rate, which ultimately resulted in the development of finer crystallites.
4. The hardness value increased from 680 to 855 Vickers by increasing carbide content from 0.9 to 2.2 wt.% in the coating.
5. The variations of the friction coefficient decreased and became more uniform, and the sliding distance increased in coated samples compared to the bare substrate.
6. Coating's corrosion resistance in 3.5 wt.% NaCl solution improved compared to the bare substrate. The corrosion resistance ranged from 2.6 kΩ.cm^2 for the bare substrate to 487 kΩ.cm^2 for the sample 18-10.

REFRENCES

[1] Torabinejad, V., Aliofkhazraei, M., Assareh, S., Allahyarzadeh, M.H., Rouhaghdam, A.S., "Electrodeposition of Ni-Fe alloys, composites, and nano coatings–A review". J. Alloys and Compounds., 2017, 691, 841-859.

[2] Raghavendra, C.R., Basavarajappa, S., Sogalad, I., "Electrodeposition of Ni-nano composite coatings: a review". J. Inorganic and Nano-Metal Chemistry., 2019, 48(12), 583-598.

[3] Mahidashti, Z., Aliofkhazraei, M., Lotfi, N., "Review of Nickel-Based Electrodeposited Tribo-Coatings". J. Transactions of the Indian Institute of Metals., 2017, 71(2), 257-295.

[4] Khorsand, S., Karbasi, M., Sayyedan, F.S., Eshaghian, M., Razavi, M., "Development of electro-co-deposited Ni–Fe(Ti,W)C nano-composite coatings". J. Surface Engineering., 2017, 34(6), 433-439.

[5] Raja, M., Ramesh Bapu, G.N.K., Maharaja, J., Sekar, R., "Electrodeposition and characterisation of Ni–TiC nanocomposite using Watts bath". J. Surface Engineering., 2014, 30(10), 697-701.

[6] Di Bari, G.A., "Electrodeposition of nickel". J. Modern electroplating., 2000, 5, 79-114.

[7] Dordsheikh Torkamani, A., Velashjerdi, M., Abbas, A., Bolourchi, M., Maji, P., "Electrodeposition of Nickel matrix composite coatings via various Boride particles: A review". J. Composites and Compounds., 2021, 3(7), 91-98.

[8] Wang, P., Cheng, Y.-l., Zhang, Z., "A study on the electrocodeposition processes and properties of Ni–SiC nanocomposite coatings". J. coatings technology and research., 2011, 8(3), 409-417.

[9] Kuru, H., Kockar, H., Alper, M., Karaagac, O., "Growth of binary Ni–Fe films: characterisations at low and high potential levels". J. Magnetism and Magnetic Materials., 2015, 377, 59-64.

[10] Lee, T.R., Chang, L., Chen, C.-H., "Effect of electrolyte temperature on composition and phase structure of nanocrystalline Fe–Ni alloys prepared by direct current electrodeposition". J. Surface and Coatings Technology., 2012, 207, 523-528.

[DOI: 10.22068/ijmse.3922]

[11] Pavithra, G., Hegde, A.C., "Magnetic property and corrosion resistance of electrodeposited nanocrystalline iron–nickel alloys". J. Applied Surface Science., 2012, 258(18), 6884-6890.
[12] Yousefi, E., Sharafi, S., Irannejad, A., "The structural, magnetic, and tribological properties of nanocrystalline Fe-Ni permalloy and Fe-Ni-TiO_2 composite coatings produced by pulse electro co-deposition". J. Alloys and Compounds., 2018, 753, 308-319.
[13] Nagayama, T., Yamamoto, T., Nakamura, T., Fujiwara, Y., "Properties of electro-deposited invar Fe–Ni alloy/SiC composite film". J. Surface and Coatings Technology., 2017, 322, 70-75.
[14] Ganji, M., Yousefnia, H., Seyedraoufi, Z., Shajari, Y., "The corrosion behavior of Ni–Fe and Ni–Fe–TiC nanoparticles deposited using pulse electrodeposition on low-carbon steel". J. Australian Ceramic Society., 2022, 1-13.
[15] Ledwig, P., Ratajski, T., Indyka, P., Kalemba-Rec, I., Kopia, A., Kąc, M., Dubiel, B., "Microstructure and Properties of Electrodeposited nc-TiO_2/Ni–Fe and Ni–Fe Coatings". J. Metals and Materials International., 2019, 26(6), 812-826.
[16] Torabinejad, V., Rouhaghdam, A.S., Aliofkhazraei, M., Allahyarzadeh, M., "Electrodeposition of Ni–Fe and Ni–Fe-(nano Al_2O_3) multilayer coatings". J. Alloys and Compounds., 2016, 657, 526-536.
[17] Ma, M., Sun, W.c., Zhang, Y.g., Liu, X.j., Dong, Y.r., Zi, J.y., Xiao, Y., "Effect of TiC Particles Concentration on Microstructure and Properties of Ni-TiC Composite Coatings". J. Materials Research., 2019, 22(6).
[18] Kartal, M., Buyukbayram, I., Alp, A., Akbulut, H., "Production of pulse electrodeposited Ni-TiC nanocomposite coatings". J. Materials Today: Proceedings., 2017, 4(7), 6982-6989.
[19] Zimmerman, A., Clark, D., Aust, K., Erb, U., "Pulse electrodeposition of Ni–SiC nanocomposite". J. Materials letters., 2002, 52(1-2), 85-90.
[20] Vaezi, M., Sadrnezhaad, S., Nikzad, L., "Electrodeposition of Ni–SiC nano-composite coatings and evaluation of wear and corrosion resistance and electroplating characteristics". J. Colloids and Surfaces A: Physicochemical and Engineering Aspects., 2008, 315(1-3), 176-182.
[21] Ataee-Esfahani, H., Vaezi, M.R., Nikzad, L., Yazdani, B., Sadrnezhaad, S.K., "Influence of SiC nanoparticles and saccharin on the structure and properties of electrodeposited Ni–Fe/SiC nanocomposite coatings". J. Alloys and Compounds., 2009, 484(1-2), 540-544.
[22] Amadeh, A., Rahimi, A., Farshchian, B., Moradi, H., "Corrosion behavior of pulse electrodeposited nanostructure Ni-SiC composite coatings". J. Nanosci Nanotechnol., 2010, 10(8), 5383-5388.
[23] Gyftou, P., Pavlatou, E.A., Spyrellis, N., "Effect of pulse electrodeposition parameters on the properties of Ni/nano-SiC composites". J. Applied Surface Science., 2008, 254(18), 5910-5916.
[24] Moravej, M., Amira, S., Prima, F., Rahem, A., Fiset, M., Mantovani, D., "Effect of electrodeposition current density on the microstructure and the degradation of electroformed iron for degradable stents". J. Materials Science and Engineering., 2011, 176(20), 1812-1822.
[25] Gamboa-Aldeco, M.E., Gale, R.J., A Guide to Problems in Modern Electrochemistry 1: 1: Ionics, Springer Science & Business Media, 2011.
[26] Xia, F., Li, Q., Ma, C., Liu, W., Ma, Z., "Preparation and wear properties of Ni/TiN–SiC nanocoatings obtained by pulse current electrodeposition". J. Ceramics International., 2020, 46(6), 7961-7969.
[27] Gül, H., Kılıç, F., Uysal, M., Aslan, S., Alp, A., Akbulut, H., "Effect of particle concentration on the structure and tribological properties of submicron particle SiC reinforced Ni metal matrix composite (MMC) coatings produced by electrodeposition". J. Applied Surface Science., 2012, 258(10), 4260-4267.
[28] Hou, K., Ger, M., Wang, L., Ke, S., "The wear behaviour of electro-codeposited Ni–SiC composites". J. Wear., 2002, 253(9-10), 994-1003.
[29] Spyrellis, N., Pavlatou, E.A., Spanou, S., Zoikis-Karathanasis, A., "Nickel and nickel-phosphorous matrix composite electro-coatings". J. Transactions of Nonferrous Metals society of China., 2009, 19(4), 800-804.
[30] Oliver, W.C., Pharr, G.M., "Measurement of hardness and elastic modulus by instrumented

[DOI: 10.22068/ijmse.3922]

indentation: Advances in understanding and refinements to methodology". J. materials research., 2004, 19(1), 3-20.

[31] Lee, H.K., Lee, H.Y., Jeon, J.M., "Codeposition of micro-and nano-sized SiC particles in the nickel matrix composite coatings obtained by electroplating". J. Surface and Coatings Technology., 2007, 201(8), 4711-4717.

[32] Beltowska-Lehman, E., Indyka, P., Bigos, A., Szczerba, M.J., Kot, M., "Ni–W/ZrO_2 nanocomposites obtained by ultrasonic DC electrodeposition". J. Materials & design., 2015, 80, 1-11.

[33] Abdel-Karim, R., Reda, Y., Muhammed, M., El-Raghy, S., Shoeib, M., Ahmed, H., "Electrodeposition and Characterization of Nanocrystalline Ni-Fe Alloys". J. Nanomaterials., 2011, 1-8.

[34] Gyftou, P., Pavlatou, E., Spyrellis, N., "Effect of pulse electrodeposition parameters on the properties of Ni/nano-SiC composites". J. Applied surface science., 2008, 254(18), 5910-5916.

[35] Frade, T., Bouzon, V., Gomes, A., da Silva Pereira, M., "Pulsed-reverse current electro-deposition of Zn and Zn-TiO_2 nano-composite films". J. Surface and Coatings Technology., 2010, 204(21-22), 3592-3598.

[36] Zhang, Z., Jiang, C., Cai, F., Fu, P., Ma, N., Ji, V., "Two stages for the evolution of crystallite size and texture of electro-deposited Ni–ZrC composite coating". J. Surface and Coatings Technology., 2015, 261, 122-129.

[37] Wei, H.J., Sun, W.C., Hou, G.Q., Zhang, F., Shi, Q., "Application of Artificial Neural Networks to Optimize Processing-Properties of Ni-TiC Composite Coatings". J. Materials Science Forum., 2015, Trans Tech Publ, pp 725-730.

[38] Sajjadnejad, M., Haghshenas, S.M.S., Badr, P., Setoudeh, N., Hosseinpour, S., "Wear and tribological characterization of nickel matrix electrodeposited composites: A review". J. Wear., 2021, 486-487.

[39] Mo, T., Chen, J., Bai, W., Wu, Y., Zhang, P., Zheng, B., "Ni/TiC composite electro-deposition on the surface of Ni-based superalloy". J. Surface and Coatings Technology., 2021, 424.

[40] Jenczyk, P., Gawrońska, M., Dera, W., Chrzanowska-Giżyńska, J., Denis, P., Jarząbek, D.M., "Application of SiC particles coated with a protective Ni layer for production of Ni/SiC co-electrodeposited composite coatings with enhanced tribological properties". J. Ceramics International., 2019, 45(17), 23540-23547.

[41] Fayyaz, O., Khan, A., Shakoor, R., Hasan, A., Yusuf, M.M., Montemor, M., Rasul, S., Khan, K., Faruque, M., Okonkwo, P.C., "Enhancement of mechanical and corrosion resistance properties of electrodeposited Ni–P–TiC composite coatings". J. Scientific Reports., 2021, 11(1), 1-16.

[DOI: 10.22068/ijmse.3922]